



Study on connecting tube dynamics for transient pressure measurement

H YADAV¹, A VENUGOPAL², S V PRABHU¹ and AMIT AGRAWAL^{1,*}

¹Department of Mechanical Engineering, Indian Institute of Technology Bombay, Powai, Mumbai 400076, India

²School of Mechanical Sciences, Indian Institute of Technology Bhubaneswar, Bhubaneswar 751013, India
e-mail: amit.agrawal@iitb.ac.in

MS received 13 October 2017; revised 31 August 2019; accepted 2 January 2020

Abstract. The present study evaluates the dynamic response of connecting tubes for transient pressure measurement. A systematic study is conducted to quantify the amplitude and phase distortion of connecting tubes of diameter 1, 2 and 3 mm with different lengths (10–50 cm). The experimental measurements and theoretical predictions have been carried out with both air and water as the working medium to cover a wide range of frequencies. The study highlights the underdamped nature of all the systems studied. The natural frequency of the system increases with an increase in the tube diameter and a decrease in tube length. The difference in natural frequency obtained from the experimental results and theoretical prediction is less for the smaller tube diameter ($d = 1$ mm) and more pronounced for the larger tube diameter. Larger tube diameters are recommended to avoid amplitude and phase distortion errors, especially in the low-frequency range. However, resonance effects are more pronounced for larger tube diameters. The phase response of larger tube diameters remains close to zero over a large range of frequency (0–0.8 times the natural frequency); hence, this range is more suitable for applications where phase information is more important than amplitude. This study is useful for compensating the amplitude and phase distortion error encountered in transient pressure measurements.

Keywords. Tube dynamics; phase drift; amplitude distortion; damping.

1. Introduction

In the modern era where the technologies are becoming more and more sophisticated the demand for accurate and precise measurement is on a surge. The pressure is one of the primary quantities which is monitored in various applications ranging from aerospace to biological systems. In aerospace application, the design of the structures for wind loads is mainly accomplished using static pressure measurements. However, the boundary layer separation leads to vortex shedding which is responsible for periodic pressure fluctuations [1]. Monitoring of these pressure fluctuations is helpful in ascertaining the state of the boundary layer (laminar/turbulent) which can help in better design with reduced drag forces and hence, high efficiency. Monitoring of transient pressure on the surfaces of buildings, chimney, bridges, etc. is also essential to avoid resonance and hence catastrophic failures. In process industries, transient pressure monitoring is practiced to avoid pressure buildup which may lead to leakage of precious process fluids. In biological applications, transient pressure

measurements are equally important to measure blood pressure, intra-cranial pressure, pressure in the lungs, etc.

Preserving the magnitude and phase of the pressure signal is challenging due to the non-ideal dynamics of the connecting tube and the pressure sensor. This problem can be avoided by flush mounting the pressure sensor with the surface. However, this simple requirement becomes difficult to fulfill in applications where space constraints are stringent, or when the transducer cannot be directly exposed to the process fluid. Hence, the study of connecting tube dynamics is essential for real-life applications. The connecting tube can significantly attenuate the signal in a certain frequency range due to viscous effects. Moreover, near the resonance frequency, the amplitude increases significantly. Phase information is particularly essential when simultaneous pressure measurements using multiple probes are required, and not measuring it carefully can cause significant error in phase averaged data.

The theoretical aspects of propagation of pressure waves in fluids in cylindrical tubing have been reviewed by Tijdeman [2]. Early theoretical and experimental works on the dynamic response of pressure measuring system here carried out by Berg and Tijdeman [3] and Iberall [4].

*For correspondence

However, these works are not able to predict the tube dynamics for an arbitrary pressure change. Whitmore [5] and Whitmore and Leondes [6] developed a complex wave mathematical model based on the unsteady Navier–Stokes equations for arbitrary changes in the input pressure. Irwin *et al* [7] proposed a transfer function based approach to correct the distortions caused by the connecting tube. Taback [8] used analogues from electrical system to predict the response of the pressure measuring system with attenuation constant being determined experimentally. This attenuation constant was used to determine the wave propagation velocity in the Rayleigh formula. Holmes and Lewis [9] provided a theoretical prediction of the distortion effect and its connection to the dynamics of the connecting tube. They mentioned that getting rid of the distortion effect requires a very accurate measure of the connecting tube geometrical parameters and the pressure sensor cavity volume. However, in most of the practical applications, the pressure sensor cavity volume is not known. Hence, theoretical predictions show a discrepancy with respect to experimental results suggesting a further careful study of the problem.

Studying the tube dynamics effect will be particularly helpful where measurements of pulsating flows are undertaken using a combination of orifice plate/venturi meter and pressure sensor [10–13]. The accuracy of Coriolis flowmeter employed for measuring such unsteady flows depends upon the natural frequency of the connecting tube and the accurate measurement of phase difference between the signals at inward and outward halves of the flow tube [14]. Study of tube dynamics will further be useful to correct measurement of the time dependent pressure distribution in unsteady aerodynamics and in pulsatile flow encountered in an internal combustion engine. For intake and exhaust flows in engines, a better understanding of the tubing system can provide accurate time-resolved measurements of the mass flow distribution under both steady and pulsating flow conditions.

The literature survey showed that several issues related to the modelling of amplitude and phase distortion still remain. The aforementioned issues provided the motivation for undertaking this work. The primary objective of this study is to determine the effect of the connecting tube on transient pressure measurement over a large parameter range involving different connecting tube diameters (1, 2, and 3 mm) and lengths (10, 20, 30, 40, and 50 mm) and spanning a large range of frequency. The dimensions of the connecting tube are chosen based on space constraints encountered in typical applications in flowmeters, pressure monitoring in microchannels, electronic cooling types of equipment, wind and water tunnel studies, etc. In the majority of the cases, the pressure values are only a few mbar high and a long connecting tube may cause significant distortion to the transient pressure signal.

2. Experimental set-up

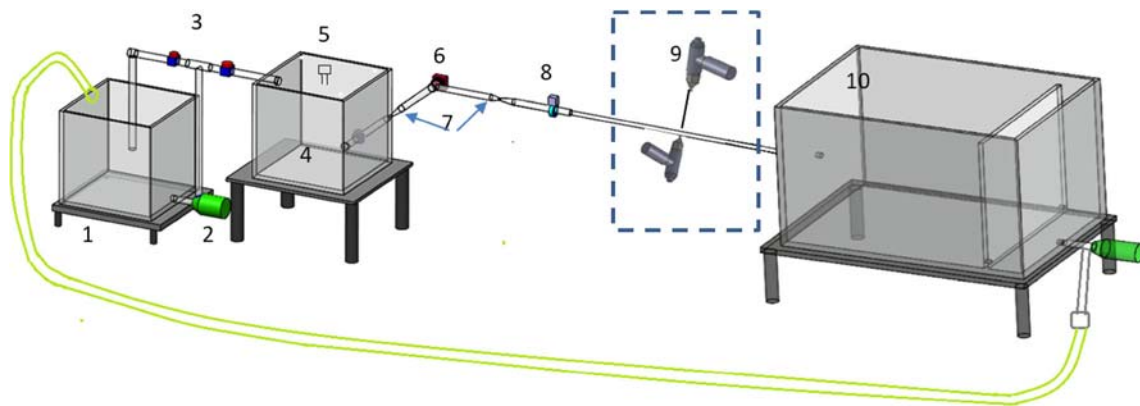
In the present study, two different working fluids (air and water) are used to cover a wide range of frequencies. The pressure pulsations in the air are generated using a synthetic jet. A solenoid valve in conjunction with a pulse driver is used to generate pressure pulsations in water. High frequency pressure pulsations are usually encountered in aerodynamics and applications where the velocity of the flow is relatively high. In most of the hydrodynamics applications, the flow velocity is low and pressure pulsations are in the relatively low-frequency range. Therefore, covering a wide range of driving frequency on amplitude amplification/attenuation is relevant and undertaken in this study.

2.1 Experimental set-up for water-based measurements

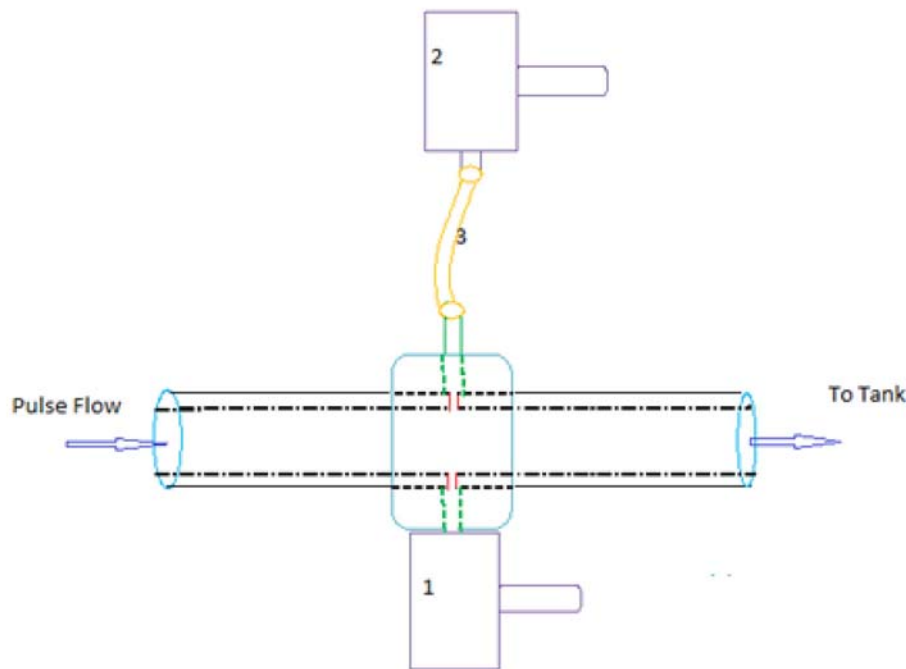
The measurement of the dynamic characteristic of a connecting tube requires a source of transient pressure, a reference sensor and a second sensor with the connecting tube. The pressure pulsations in water are generated by a solenoid valve operated by a pulse driver. The pressure response is measured with a piezo-resistive type pressure sensor (UNIK[®] 5000), with a frequency response of 5 kHz, pressure range of 0–350 mbar and accuracy 0.04% of full scale. The frequency range covered in the present experiments with water as a working fluid is 0.5–32 Hz. The schematic of the connection of pressure sensors is shown in figure 1a. Water is pumped through a 2 meter long, 8 mm diameter acrylic pipe as shown in figure 1b. The reference sensor (1) is directly flush mounted on the surface of the pipe, while the second sensor (2) is connected with a help of connecting tube and located diametrically opposite to the reference sensor. The measurements are carried out in a fully developed turbulent pipe flow regime. The Reynolds number of the flow is 12,000.

Experiments are carried out for three different diameters of silicon tube (1 mm, 2 mm, 3 mm), and five different sets of tube length (10–50 mm, with an increment of 10 mm). The overall arrangement of the experimental setup comprises a water storage tank, a settling chamber, two pumps, solenoid valve, tube, pressure gauge, pulse driver, magnetic flow meter, transient pressure sensor.

The pressure sensor and venturi meter measure the average flow rate. Water is pumped into the settling tank from the storage tank to remove fluctuations from the pump. A pressure gauge is mounted on the settling tank to ensure that the pressure is constant during the experiments. A pulse driver is used to induce pulsations in the flow using the solenoid valve. The complete arrangement ensures that the pressure pulsations are generated only by the solenoid valve.



(a)



(b)

Figure 1. (a) Schematic of experimental setup with solenoid valve assembly used for water based measurements. (1) Reservoir tank, (2) Pump, (3) Gate Valve, (4) Settling tank, (5) Pressure gauge, (6) Solenoid valve, (7) Venturi meter, (8) Flow meter, (9) Pressure sensor, (10) Collecting tank. (b) Zoomed view of pressure sensor connection with acrylic tube with water as working fluid. (1) Reference sensor, (2) Second sensor, (3) Connecting tube.

2.2 Experimental set-up for air-based measurements

To measure the effect of tube dynamics with air as the working medium and effect of the higher frequency range, further experiments are conducted with a speaker within a cavity. The pressure is synthesized using a synthetic jet operating through an acoustic speaker. The synthetic jet

creates a mean fluid motion that is generated by a sufficient strong oscillatory flow through an orifice or nozzle during an oscillatory process of suction and blowing between a synthetic jet diaphragm cavity and its surroundings. A circular cavity is mounted on top of the speaker. The speaker is excited with a signal generator capable of producing voltage signals of varying frequency and amplitude. The details about the construction of synthetic jet is

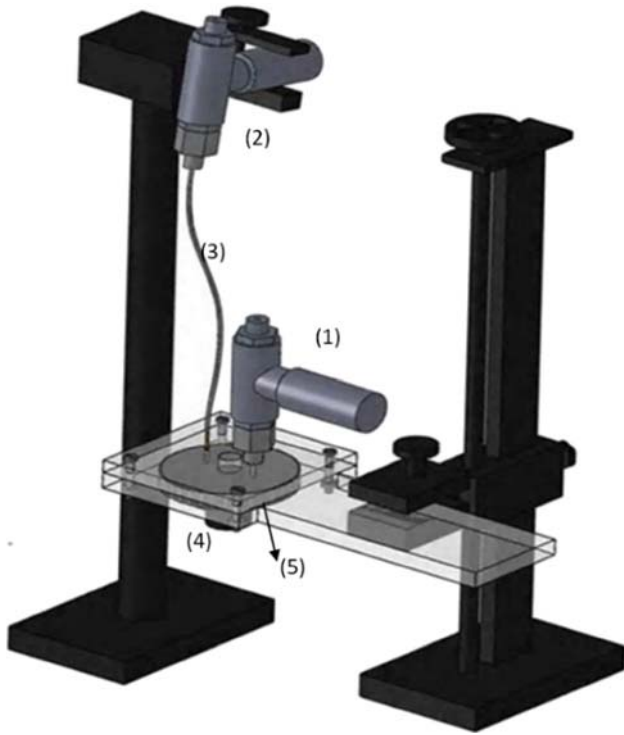


Figure 2. Schematic of experimental setup: (1) reference sensor, (2) second sensor, (3) connecting tube, (4) loudspeaker, (5) synthetic jet with cavity.

provided in the literature [15]. The schematic of the present setup is shown in figure. 2. The reference sensor is mounted directly on the jet cavity plate while the second sensor connected with a tube is mounted symmetrically opposite to the first sensor as shown in figure 2. The pressure sensors are piezo-resistive (UNIK 5000) type with a frequency response of 5 kHz and a pressure range of 0–68 mbar. The frequency range covered in this experiment is 20–500 Hz. The synthetic jet is actuated for various amplitudes; however, the results are found to be invariant of operating amplitude over the range tested. Hence, all of the results are reported with an excitation voltage of 1 V peak-to-peak. This voltage level generates sufficient pressure inside the cavity to be measured with the pressure sensors. The connecting tubes are made up of silicon which are typically used for pneumatic connections in low pressure applications.

3. Model of the system

A simple pressure system consisting of a pressure tap and remotely connected with a pressure sensor is shown in figure 3. The dynamic pressure is measured with a diaphragm type pressure sensor, whose response can be modelled as a second order system [16]:

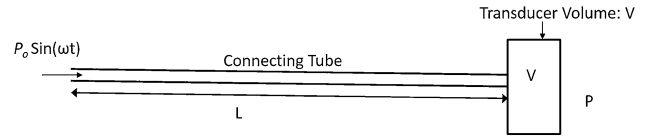


Figure 3. Schematic of connecting tube and transducer volume.

$$\frac{d^2P}{dt^2} + 2\zeta\omega_n \frac{dP}{dt} + \omega_n^2 P = K\omega_n^2 P_0 \quad (1)$$

where, $P_0(t)$ is the desired unsteady pressure at a surface port, which is connected to the remotely mounted pressure transducer with a diameter D and length of tubing L . The pressure measured by the pressure transducer is denoted $P(t)$, ζ is the damping factor, ω_n is the natural frequency ($2\pi f_n$) and K is the static gain.

The steady state response of the second order system to a sinusoidal input is [16]:

$$P = \frac{KP_0}{\left[(1 - \omega^2/\omega_n^2)^2 + (2\zeta\omega/\omega_n)^2 \right]^{1/2}} \sin(\omega t + \phi) \quad (2)$$

where ω is the operating frequency and phase lag ϕ is given as

$$\phi = \tan^{-1} \left(-\frac{2\zeta\omega/\omega_n}{1 - \omega^2/\omega_n^2} \right) \quad (3)$$

Assuming static gain is unity in Eq. (1) and comparing with a second order equation derived from the Navier–Stokes equation by Whitmore and Leondes [6], we obtain

$$\omega_n = c\sqrt{\frac{A_c}{LV}}; \quad \omega_n \propto \frac{D}{\sqrt{L}} \quad (4)$$

$$\zeta = \frac{16\mu}{D^2\rho\omega_n}; \quad \zeta \propto \frac{\sqrt{L}}{D^3} \quad (5)$$

where, A_c , D are the internal cross-section area and diameter of the connecting tube respectively, V is the volume of the transducer, μ , ρ represent dynamic viscosity and density of the medium respectively, and c is the speed of sound. Equation (4) is used to predict the natural frequency for compressible fluid (air) [17]. The equation suggests that with an increase in the tube diameter the natural frequency of the system increases while with an increase in the tube length the natural frequency of the system reduces.

For liquid filled system the natural frequency f_n of the system is determined by an equation given by Anderson and Englund [18]:

$$f_n = \frac{a}{4L} \sqrt{\frac{V_{TB_e}}{B(\frac{\Delta V}{\Delta P})_{TD} + V_{TD} + V_{TB_e}}} \quad (6)$$

where, a is the acoustic velocity in water, V_{TB_c} is the effective tube volume, B is the bulk modulus of water, $(\frac{\Delta V}{\Delta P})_{TD}$ is the transducer compliance, and V_{TD} is the transducer volume. Equation (5) is used to determine the damping factor for both water and air [17, 19].

The input pressure in most of the practical applications is either a sinusoidal or square wave. The solution of the analytical model (Eq. 1) depends on the value of the natural frequency and damping factor. However, it is rather difficult to estimate the value of natural frequency and damping factor accurately; hence, analytical models fail to predict the dynamic response of the connecting tube. An alternate and more precise way of estimating these factors is by experimental determination using a reference sensor.

The amplitude damping associated with the connecting tube compared to the reference sensor can be estimated either in time or in the frequency domain. In the present study, the amplitude ratio and phase drift are obtained in the time domain. The amplitude of the two signals at each crest is recorded and averaged over a sufficiently long time to obtain the average amplitude ratio. The phase drift is obtained by using the cross-correlation technique. The dominant peak in the cross-correlation function represents the time lag/phase lag between the two signals.

4. Results and discussion

4.1 Water as working medium and transient pressure generation with solenoid valve (Low frequency range)

The experimental results for different tube lengths and tube radii have been discussed in this section for water as the working medium and transient pressure generation using a solenoid valve. The pressure variation at the surface is transmitted through the connecting tube to the transducer. The pressure variation propagates as a wave. An ingoing pressure wave (upstream) gets reflected from the fixed end of the transducer. This inverted wave is again reflected from the surface where the pressure has to be measured. After two reflections the wave moves towards the upstream side and interferes with the new wave. Due to friction along the wall of the connecting tube, the propagated wave attenuates in the connecting tube. The interference of the two waves either dampens or get amplified depending upon the phase difference between the two waves. The accuracy of the measurement system deteriorates significantly if the amplitude attenuation is significant. This attenuation causes a significant loss in the resolution of the measurement system especially when low resolution analog to digital converters are employed [6, 19]. The amplitudes may increase significantly if the frequency range of operation is close to the resonance frequency. This increase in amplitude may cause permanent damage to the instruments.

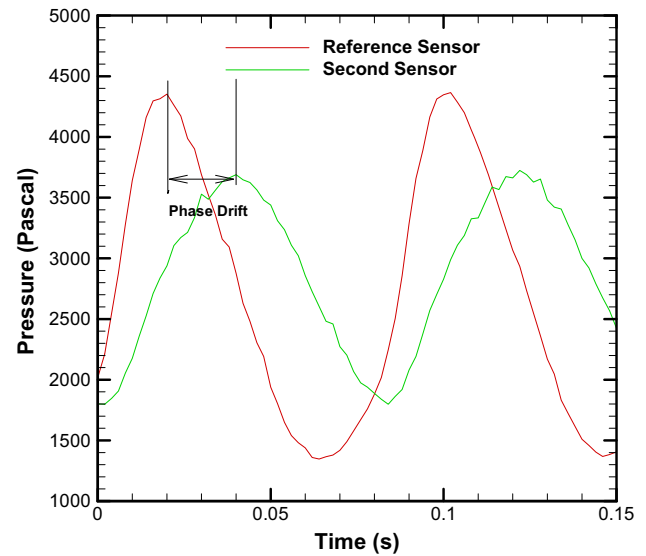


Figure 4. Time series of pressure: $L = 20$ mm, $f = 12.2$ Hz, showing the definition of phase drift and difference in measured amplitude by both sensors.

Hence, a true estimate of the amplitude response over the operating frequency range is essential.

A time series of pressure measured by both the sensors is shown in figure 4. The mean pressure value measured by the reference sensor and the second sensor is within $\pm 0.6\%$ of each other, at the lowest frequency (0.5 Hz) studied in the present case attesting to the quality of the measurements. In figure 4, the second sensor shows distortion in amplitude as compared to the reference sensor due to the connecting tube. In addition to this distortion or amplification, the signal may also lag from the reference signal. This lag or the phase drift is shown in the figure, which indicates the fraction of a period that the measured signal lags the actual signal.

The signals of pressure fluctuation are recorded by pressure transducers (both reference sensor and second sensor) at 500 sampling rates for the complete set of measurements. The power spectral density (PSD) of a signal is computed for the reference sensor and the second sensor and shown in figure 5. The PSD shows a peak value at the operating frequency as expected. Fourier transform provides the amplitude of the signal in W/Hz. A separate calculation is carried out for both the pressure sensors. A square root of ratio of the second pressure sensor to the reference pressure represents the amplitude ratio. Pressure fluctuations read by the second sensor depends upon several factors such as the length and diameter of the connecting tube, elastic expansion of the tube, compressibility of the working fluid, and attenuation caused by viscous dissipation [20]. With the difference in the tubing material, transmission characteristics of the pressure wave changes due to different surface roughness and its elastic property. For the low-pressure application, the surface roughness is

more important than the elastic property of the tube. The term low pressure implies that during the wave transmission the tube volume will remain constant (or negligible variation will occur) with a change in both applied pressure and frequency.

To predict the response of the pressure measuring system theoretically, the main difficulty is in measuring the transducer volume and change in transducer volume with change in applied pressure (due to deflection in diaphragm). The natural frequency for the different tube lengths and tube diameters is determined by using Eq. (6). The transducer volume is determined by using Eq. (4) taking the natural frequency determined by the experiment for the case of 2 mm diameter and 10 mm tube length. The same transducer volume is used for the calculation of natural frequency with both water and air. The transducer compliance is determined using Eq. (6) by taking the natural frequency of water determined from the experiment. This value of transducer compliance is subsequently kept constant for all the cases. Figure 6 shows the variation of natural frequency

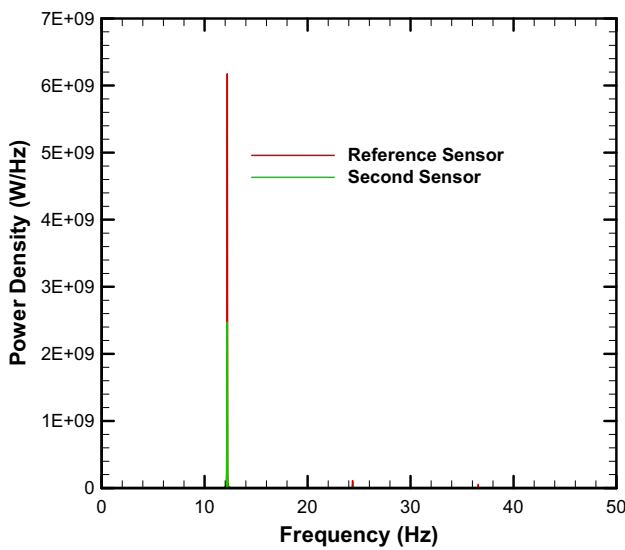


Figure 5. FFT of time series signal.

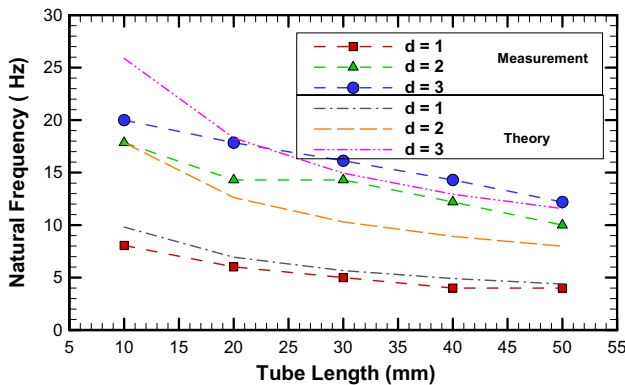


Figure 6. Variation of natural frequency with tube length

with tube length for different tube diameters. Note that for fixed tube diameter, the experimental natural frequency for different tube lengths is corresponding to the maximum pressure measured by the second pressure sensor.

Pressure measurements are carried out at a difference of 2 Hz for each case (except $d = 3$ mm; $L = 10$ mm). So the error band in the natural frequency is ± 2 Hz. Both experimental and theoretical natural frequencies are compared in the figure 6. The natural frequency corresponding to tube diameter $d = 1$ mm has a lesser deviation as compared to a tube diameter of 2 mm and 3 mm. Tube diameter $d = 2$ mm and $L = 10$ mm represents the baseline case at which the transducer compliance has been determined. The difference in experimental and theoretical results is due to the variation of transducer compliance with frequency and tube length. Figure 7 represents the percentage change in the transducer compliance with tube length for various tube diameters at their natural frequency. The change in volume per unit pressure is more for smaller tube length.

Figure 8 shows the variation of amplitude ratio with excitation frequency. The figure shows both amplified (amplitude ratio > 1) and damped signals (amplitude ratio < 1) compared to the reference signal. The figure further shows that for a fixed tube diameter as the length of the tubing increases the natural frequency of the system decreases. With an increase in the tube diameter the natural frequency of the system increases. As discussed in section 3, this result is expected because the natural frequency of the system increases linearly with an increase in the tube diameter and decreases as a square root of tube length. Figure 8 also shows that for low diameter of tube ($d = 1$ mm) signals are less distorted in magnitude (amplitude ratio ≈ 1) near to their resonance frequency compared to signal distortion for larger tube diameter ($d = 3$ mm). The signal is free of distortion in the low-frequency end, with the range being largest for a 3 mm diameter tube. These observations are relevant from a practical point of view.

Figure 9 shows the variation of amplitude ratio with normalized frequency, the frequency is normalized by the natural frequency. The theoretical amplitude ratio versus normalized frequency is also plotted in the figure. The

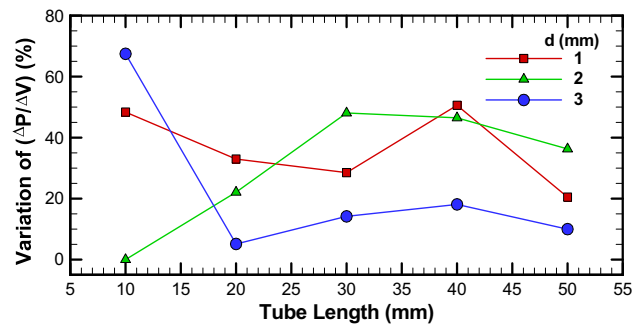


Figure 7. Change in transducer compliance with tube length.

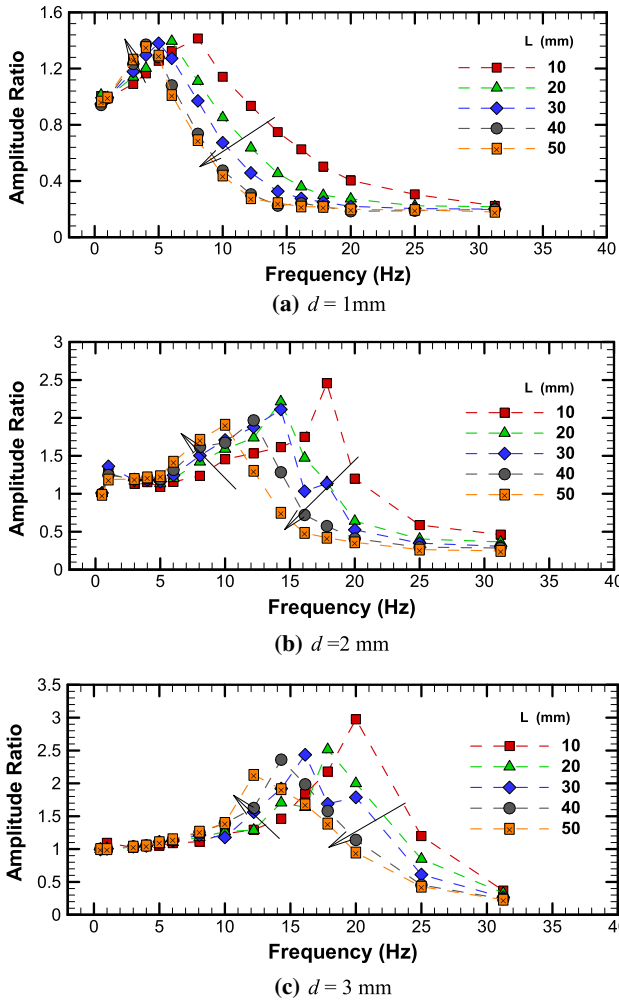


Figure 8. Amplitude ratio variation with frequency for various tube length.

theoretical amplitude ratio is determined by using Eq. (2). The figure shows that the experimental data for different tube lengths collapse on to a single curve and a slight difference in the amplitude ratio is only observed close to the natural frequency. The shape of the curves in figures 9a–c is similar, however, the peak magnitude seems to increase with an increase in tube diameter. Figure 9a shows a substantial difference between the experimental and theoretical results over the entire frequency range. This variation is due to the difference in the damping factor determined from Eq. (5). Anderson and Englund [17] reported that the theoretical damping factor differs by 100% from their experimental results. They also found that the variation in the damping factor is larger for the smaller tube diameter, as further discussed in section 4.3. Furthermore, the theoretical amplitude is determined using Eq. (2). The natural frequency in this equation requires the value of transducer volume which is determined using Eq. (4). Presumably, the error in determining the transducer volume is influenced more by the term $V_{TD} + V_{TB_c}$ used in Eq. (6)

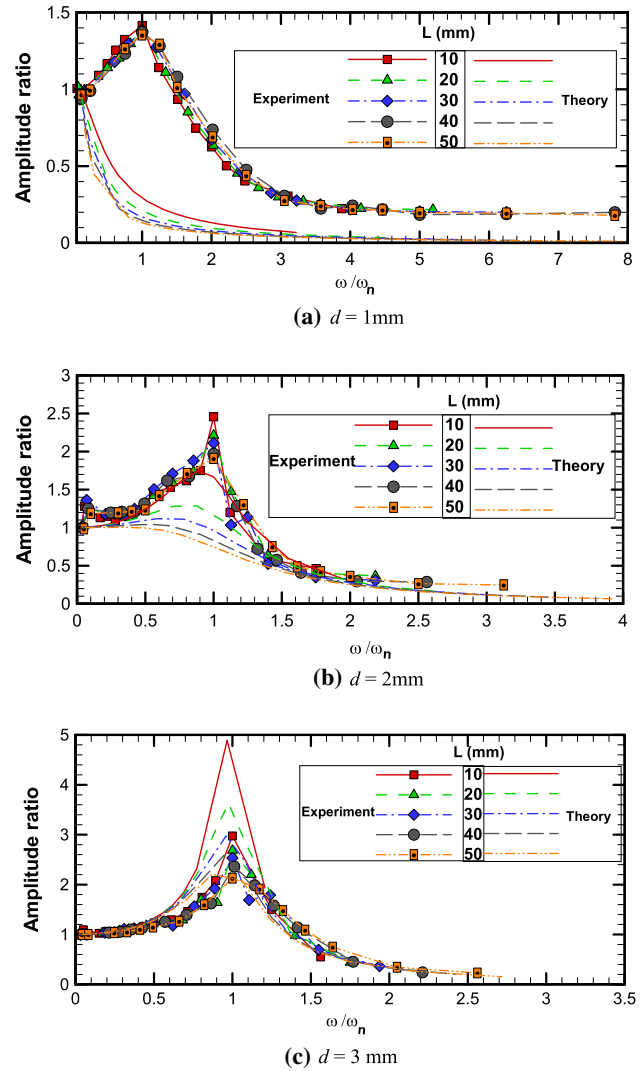


Figure 9. Normalized amplitude ratio variation with frequency for various tube lengths.

for 1 mm tube diameter compared to the other tube diameter. This error may be responsible for a substantial difference between the theoretical and experimental results seen in this case. For a tube diameter of 2 mm and 3 mm, the theoretical amplitude ratio differs only close to the natural frequency. Theoretical predictions for a tube diameter of 3 mm and 10 mm tube length differ by 64% from the corresponding experimental result at the natural frequency. The theoretical result under predicts the experimental result in the figure 9b, while it over predicts in figure 9c.

The above results show that the minimum distortion in signal occurs with 1 mm tube diameter. The result is further insensitive to the tube length. The theoretical results show a damped signal over the entire range of frequency; however, experimental results show both amplified and damped signals. Therefore, it is suggested to use the instrument close to its natural frequency with care to prevent damage to the

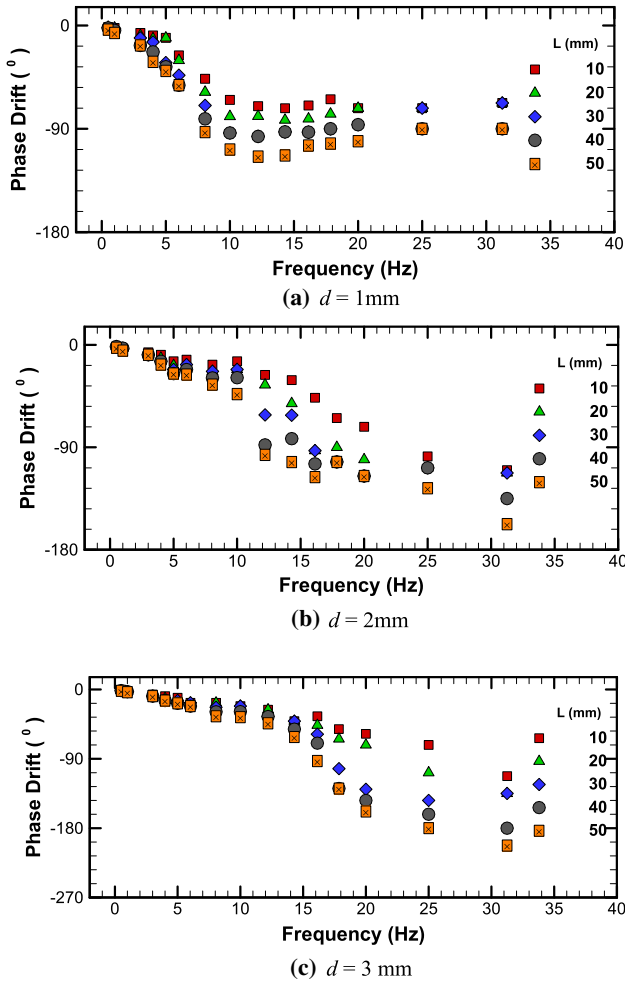


Figure 10. Phase drift variation with frequency for various tube lengths.

instrument, and utilize the full range of the instrument to minimize uncertainty in the measurement.

Figure 10 shows the phase difference between the two signals (measured and reference) at different frequencies and various tube lengths and diameters. For each diameter ($d = 1, 2, 3$ mm) of the tube, the phase difference is less and nearly constant for various tube lengths up to its natural frequency. The phase difference increases very rapidly beyond the natural frequency. For $d = 1$ mm, the phase difference becomes constant for higher frequencies due to the low natural frequency. A small tube length gives a relatively lower phase difference.

4.2 Air as working medium and transient pressure generation with acoustic actuator (High frequency range)

In this section, experimental results are presented which are carried out for higher frequency ranges (20–500 Hz) at an interval of 10 Hz which provides an error band of ± 10 Hz

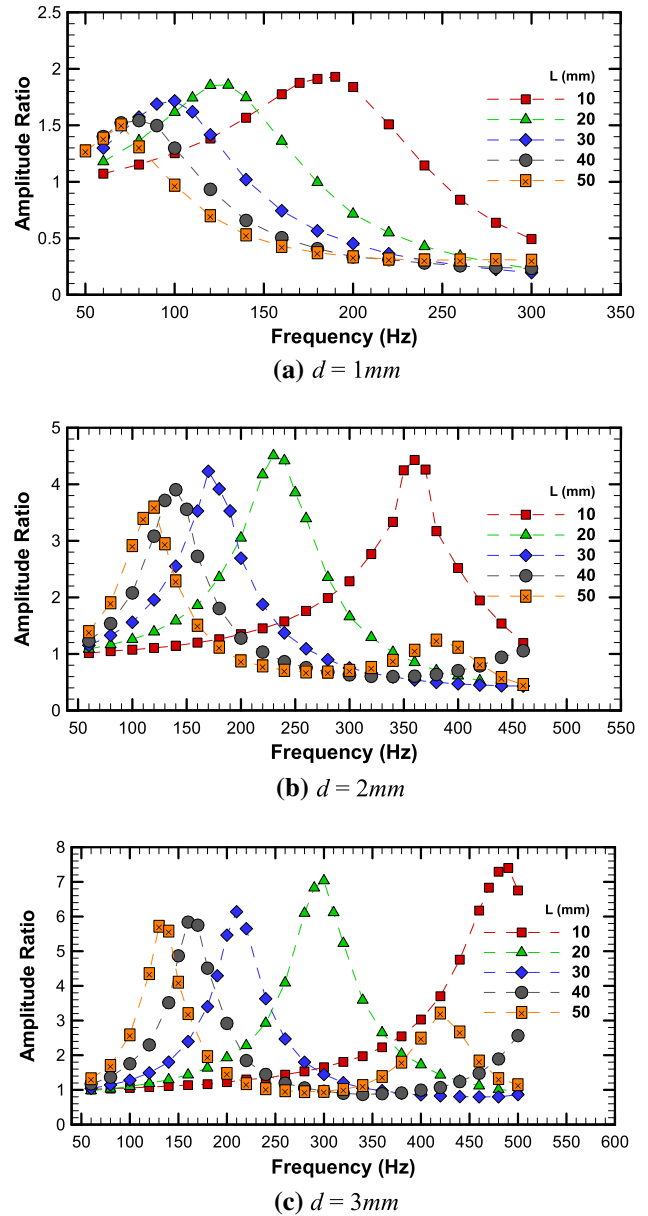


Figure 11. Amplitude ratio variation with frequency for various tube lengths.

in the measurement of the natural frequency. The higher frequencies are achieved by suction and blowing process of the diaphragm cavity. The sampling frequency, in this case, is selected as 2 kHz to ensure good resolution in phase drift estimation at high frequencies. The connecting tube dimension is the same as discussed in the previous section. The amplitude variation with the operating frequency for a tube diameter of 1, 2 and 3 mm is shown in figure 11. As described earlier, the peak in the amplitude response curve occurs at the natural frequency of the system. It is observed that upon normalization, the response curves show identical characteristics and the difference in amplitude ratio is only observed at a natural frequency

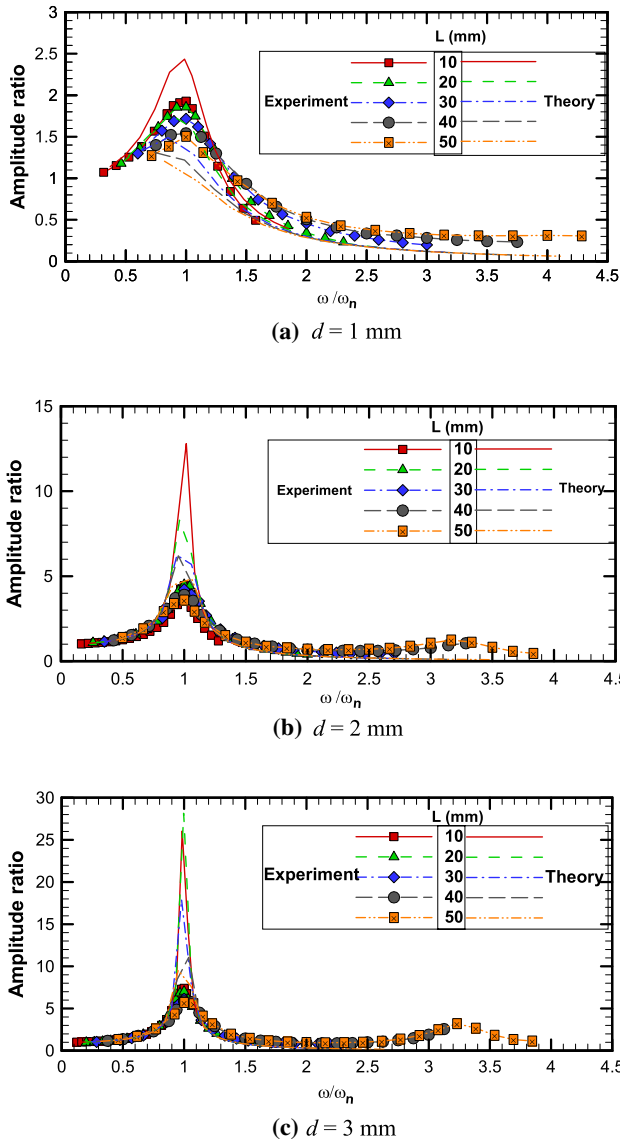


Figure 12. Normalized amplitude ratio variation with frequency for various tube lengths.

(figure 12). The figure also depicts the theoretical prediction of the amplitude ratio using Eq. (2). The theoretical predictions agree well with the experimental results away from the natural frequency; however, close to the natural frequency the predictions substantially over predict the amplitude ratio. For example, the amplitude ratio for 3 mm tube diameter is up to eight times higher than the input signal close to the resonance frequency. Pressure sensor operating over its full scale may, therefore, encounter severe implications if operated close to its resonance frequency.

The natural frequency variation with tube length for various tube diameters is shown in figure 13. A monotonous increase in natural frequency is noticed with an increase in tube diameter and a decrease in tube length. Here, the theoretical prediction of natural frequency for

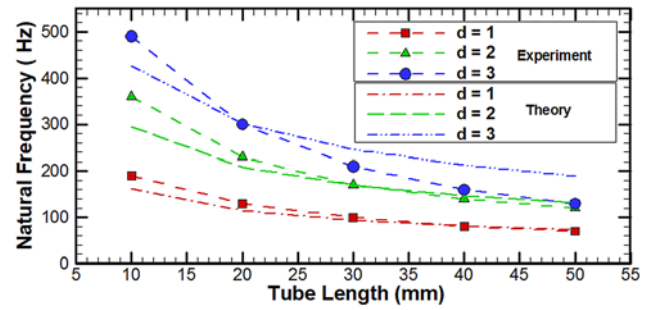


Figure 13. Natural frequency variation with connecting tube length.

1 mm tube diameter is closer to the experimental results as compared to that for 2 mm and 3 mm tube diameter. The difference in the experimental and theoretical results with tube diameter and length can be bridged by changing the transducer volume, required in the determination of natural frequency (see Eq. 4). The trends are close to the theoretical predictions suggested by Sun *et al* [21] and Whitmore *et al* [22]. The phase drift plots for various connecting tube lengths are shown in figure 14. The phase drift is close to zero for all tube diameters and tube lengths in the low frequency range. However, with an increase in frequency, significant phase drift is observed for larger lengths. The phase drift is as high as 300° for larger tube lengths. The normalized phase drift plots collapse onto a single curve for a given tube diameter as shown in figure 15. The figure also shows the theoretical prediction of phase drift with tube diameter for various tube diameters. The theoretical phase drift is determined from Eq. (3). The experimental results and theoretical predictions for phase drift match well over the tube diameter and length investigated, except for larger tube lengths of 40 mm and 50 mm in the larger excitation frequency range (2.5 times the natural frequency). It is interesting to observe that for larger tube diameters the phase drift values remain nearly close to zero till $0.8\omega/\omega_n$. However, close to the resonance frequency drastic change in phase, drifts are observed and the values tend to increase. The results highlights that larger tube diameter (3 mm) can be employed in the low frequency range ($\omega/\omega_n = 0-0.8$) to preserve the phase information. However, if the sensors are operated in the high frequency range, phase distortion is significant and needs to be corrected.

4.3 Response to step input

Figure 16 shows the time response of the tubing system. The time response of the measuring system of single degrees of freedom system can be estimated by tracking the logarithmic decay of the step response. The logarithmic decrement is related to the damping factor by the following relation [23]:

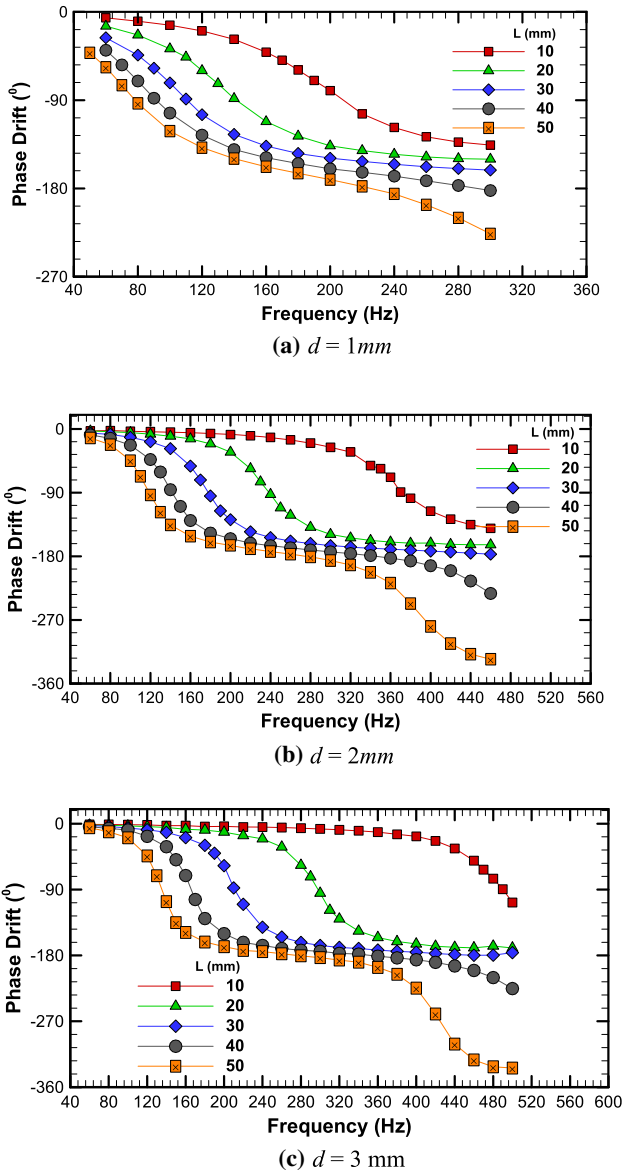


Figure 14. Phase drift variation with frequency for various tube length.

$$\ln\left(\frac{y_i}{y_{i+n}}\right) = n \frac{2\pi\xi}{\sqrt{1-\xi^2}} \quad (4)$$

where y_i is the amplitude after i cycles, and n is the number of cycles.

The damping factor for various tube lengths and its internal diameter is shown in figure 17. The damping ratio is found to increase with a decrease in tube diameter and an increase in the tube length. Further, the damping factor is more sensitive to length compared to the tube diameter and follows a nonlinear trend. The characteristics resemble an under damped system. The under damped system can also be described based on settling time. The settling time is defined as the time required for the output to reach and remain within $\pm 1\%$ of the total change in output. As shown

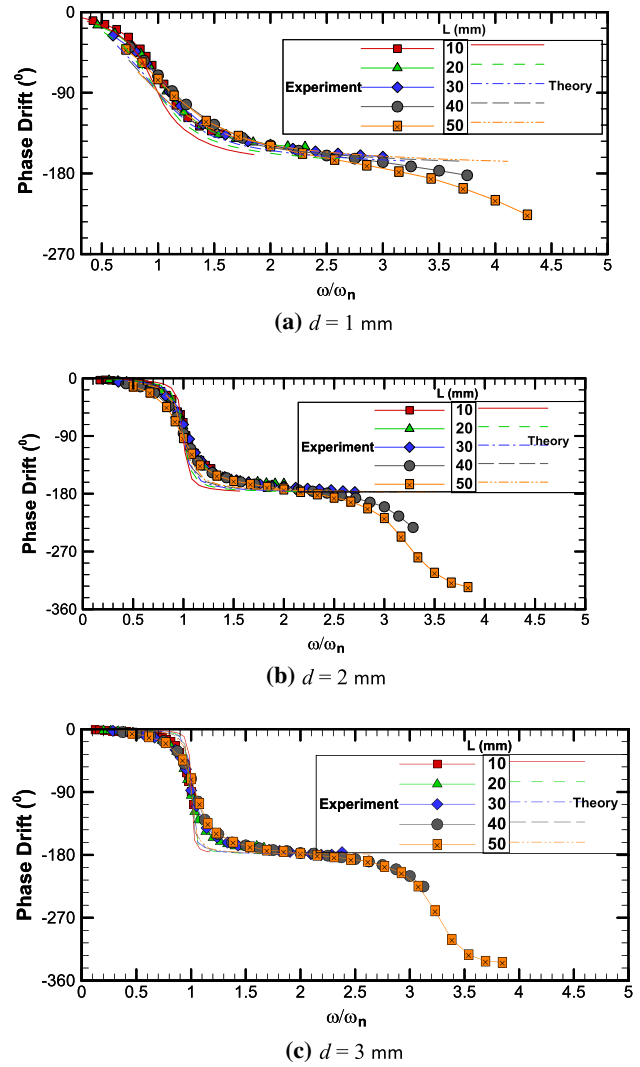


Figure 15. Normalized amplitude ratio variation with frequency for various tube length.

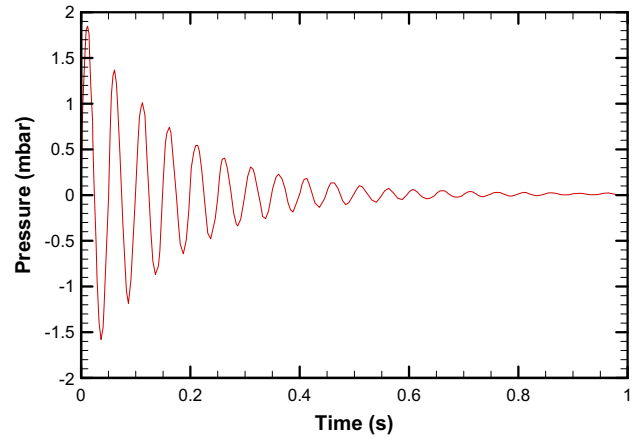


Figure 16. Logarithmic decay of pressure signal for step input.

in figure 18, the settling time increases with an increase in the connecting tube length. It is interesting to note that the settling times for 2 mm and 3 mm tube diameter are almost

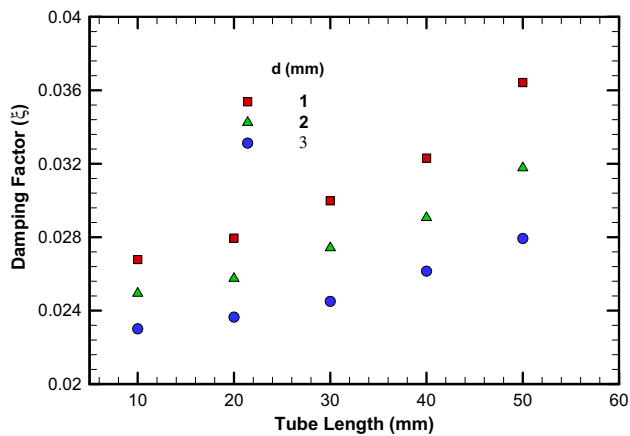


Figure 17. Damping factor variation with connecting tube length.

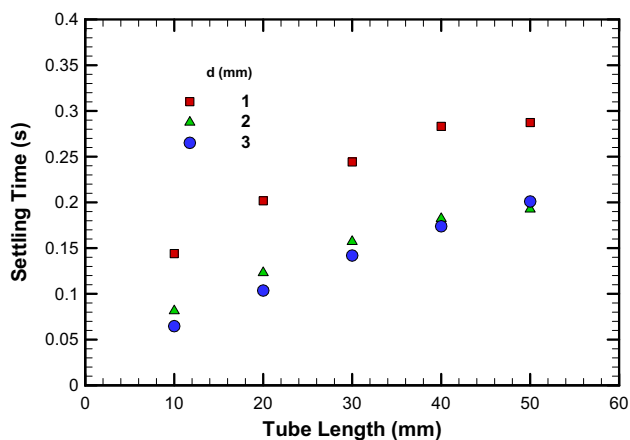


Figure 18. Variation of settling time with connecting tube length.

identical. The settling time for larger diameter and smaller length have a smaller value. So the selection for faster response time for transient pressure measurement will be larger tube diameter and smaller length. Irwine *et al* [7] suggested that the connecting tube should have an optimum range of diameter. Their results show that the increased diameter is not so critical. However, our result indicates that the response time increases rapidly for tube diameter of 1 mm.

5. Conclusions

An experimental and theoretical parametric study is conducted on the connecting tube dynamics for transient pressure measuring. The pressure sensors employed in the present study are a piezo resistive type with a frequency response of 5 kHz. Connecting tube diameters 1, 2 and 3 mm with different lengths 10, 20, 30, 40 and 50 mm are evaluated for the transient characteristics.

1. It is observed that the natural frequency of the system increases with an increase in tube diameter and decreases with the tube length. The theoretical prediction of natural frequency for both water and air is close to the experimental result for 1 mm tube diameter; however, the difference is more for 2 mm and 3 mm tube diameter cases. The difference is attributed to a change in the transducer volume with frequency.
2. The experimental results can be predicted using a simple 2nd order model. However, the value of the model (damping and natural frequency) are rather difficult to obtain from theory.
3. The normalized amplitude plots collapse onto a single curve with a reduction in amplitude observed close to the resonance frequency. The phase drift shows a significant deviation in the higher frequency range, especially for larger (3 mm) tube diameter. It is interesting to observe that for larger tube diameters the phase drift values remain nearly close to zero till $0.8\omega/\omega_n$. All of the systems studied showed characteristics of an under-damped system. These results are particularly useful for transient pressure measurement for correcting the amplitude and phase distortion.
4. A smaller tube diameter picks the amplitude better and also leads to a smaller phase lag.
5. To measure the correct input signal, the natural frequency of the connecting tube and transducer should be greater than the input signal [24]. The result presented showed the natural frequency for two different mediums (air and water) and different tube lengths and diameter. These natural frequencies can be used to measure up to the upper limit of input signal correctly, using a proper combination of tube length and diameter. Other combinations except presented here can also be used with proper calibration procedure of connecting tube with a transducer.

References

- [1] Schlichting H 1979 *Boundary-Layer Theory*. McGraw-Hill, New York
- [2] Tijdeman H 1975 On the propagation of sound waves in cylindrical tubes. *J. Sound Vib.* 39(1): 1–33
- [3] Bergh H and Tijdeman H 1965 *Theoretical and Experimental Results for the Dynamic Response of Pressure Measuring Systems*. National Aeronautical and Astronautical Research Institute, Amsterdam, NLR-TR F 238
- [4] Iberall A S 1950 Attenuation of Oscillatory Pressures in Instrument Lines. *Journal of Research of the National Bureau of Standards* 45: No. NBS-RP-2115
- [5] Whitmore S A 1988 Formulation of a general technique for predicting pneumatic attenuation errors in airborne pressure sensing devices. *National Aeronautics and Space Administration Technical Memorandum: 2085*
- [6] Whitmore S A and Leondes C T 1990 Compensating for pneumatic distortion in pressure sensing devices. *National Aeronautics and Space Administration Technical Memorandum: 631*

- [7] Irwin H P A H, Cooper K R and Girard R 1979 Correction of distortion effects caused by tubing systems in measurements of fluctuating pressures. *J. Wind Eng. Ind. Aerodyn.* 5(1): 93–107
- [8] Taback I 1949 The response of pressure measuring systems to oscillating pressures. *National Advisory Committee for Aeronautics: NACA Technical Note No. 1819*
- [9] Holmes J D and Lewis R E 1987 Optimization of dynamic-pressure-measurement systems. I. Single point measurements. *J. Wind Eng. Ind. Aerodyn.* 25(3): 249–273
- [10] Doblhoff-Dier K, Kudlaty K, Wiesinger M and Gröschl M 2011 Time resolved measurement of pulsating flow using orifices. *Flow Meas. Instrum.* 22(2): 97–103.
- [11] Shaaban S 2017 Design and optimization of a novel flowmeter for liquid hydrogen. *Int. J. Hydrogen Energy* 42(2):14621–14632
- [12] Steven R N 2002 Wet gas metering with a horizontally mounted Venturi meter. *Flow Meas. Instrum.* 12(5): 361–372
- [13] Yadav H, Agrawal A and Srivastava A 2016 Mixing and entrainment characteristics of a pulse jet. *Int. J. Heat Fluid Flow* 61: 749–761
- [14] Svete A, Kutin J, Bobovnik G and Bajsić I 2015 Theoretical and experimental investigations of flow pulsation effects in Coriolis mass flowmeters. *J. Sound Vib.* 352: 30–45
- [15] Chaudhari M, Verma G, Puranik B and Agrawal A 2009 Frequency response of a synthetic jet cavity. *Exp. Therm. Fluid Sci.* 33(3): 439–448
- [16] Coleman H W and Steele W G 2009 *Experimentation, Validation, and Uncertainty Analysis for Engineers*. Wiley, Hoboken
- [17] Bajsić I, Jože K and Žagar T 2007 Response time of a pressure measurement system with a connecting tube. *Instrum. Sci. Technol.* 35(4): 399–409
- [18] Anderson R C and Englund D R 1971 Liquid-filled transient pressure measuring systems: A method for determining frequency response. *National Aeronautics and Space Administration Technical Memorandum: TN-D-6603*
- [19] Gerstoft P and Hansen S O 1987 A new tubing system for the measurement of fluctuating pressures. *J. Wind Eng. Ind. Aerodyn.* 25(3): 335–354
- [20] Hurst A M and Van DeWeert J 2013 An experimental and theoretical investigation of wave propagation in teflon and nylon tubing with methods to prevent aliasing in pressure scanners. *J. Eng. Gas Turb. Power* 135(10): 101602
- [21] Sun Z, Zhang H and Zhou J 2007 Investigation of the pressure probe properties as the sensor in the vortex flowmeter. *Sens. Actuators A Phys.* 136(2): 646–655
- [22] Whitmore S A and Cornelius T L 1991 Pneumatic distortion compensation for aircraft surface pressure sensing devices. *J. Aircr.* 28(12): 828–836
- [23] Burton T D 1994 *Introduction to Dynamic Systems Analysis*. McGraw-Hill, New York
- [24] Holman J P 1994 *Experimental Methods for Engineers*, 6th Edition, McGraw Hills, New York